

This is a self-archived version of an original article. This version may differ from the original in pagination and typographic details.

Author(s): Moghadam, N.N.; Sidhu, K.; Summanen, P.A.M.; Ketola, T.; Kronholm, I.

Title: Quantitative genetics of temperature performance curves of *Neurospora crassa*

Year: 2020

Version: Accepted version (Final draft)

Copyright: © The Author(s)


Rights: CC BY 4.0

Rights url: <https://creativecommons.org/licenses/by/4.0/>

Please cite the original version:

Moghadam, N.N., Sidhu, K., Summanen, P.A.M., Ketola, T., & Kronholm, I. (2020). Quantitative genetics of temperature performance curves of *Neurospora crassa*. *Evolution*, 74(8), 1772-1787. <https://doi.org/10.1111/evo.14016>

Quantitative genetics of temperature performance curves of *Neurospora crassa*

Neda N. Moghadam,¹ Karendeep Sidhu,¹ Pauliina A. M. Summanen,¹ Tarmo Ketola,¹
 and Ilkka Kronholm^{1,2} 

¹Department of Biological and Environmental Science, University of Jyväskylä, Jyväskylä FI-40014, Finland

²E-mail: ilkka.kronholm@jyu.fi

Received January 22, 2020

Earth's temperature is increasing due to anthropogenic CO₂ emissions; and organisms need either to adapt to higher temperatures, migrate into colder areas, or face extinction. Temperature affects nearly all aspects of an organism's physiology via its influence on metabolic rate and protein structure, therefore genetic adaptation to increased temperature may be much harder to achieve compared to other abiotic stresses. There is still much to be learned about the evolutionary potential for adaptation to higher temperatures, therefore we studied the quantitative genetics of growth rates in different temperatures that make up the thermal performance curve of the fungal model system *Neurospora crassa*. We studied the amount of genetic variation for thermal performance curves and examined possible genetic constraints by estimating the G-matrix. We observed a substantial amount of genetic variation for growth in different temperatures, and most genetic variation was for performance curve elevation. Contrary to common theoretical assumptions, we did not find strong evidence for genetic trade-offs for growth between hotter and colder temperatures. We also simulated short-term evolution of thermal performance curves of *N. crassa*, and suggest that they can have versatile responses to selection.

KEY WORDS: Evolvability, fungi, G-matrix, phenotypic plasticity, reaction norm.

Earth's temperature is rising due to anthropogenic activities (IPCC 2013). The challenge most organisms will face in a warming world is that they have to either adapt to warmer conditions or migrate into colder areas to avoid extinction (Deutsch et al. 2008; Dillon et al. 2010; Araújo et al. 2013; Merilä and Hendry 2014). Temperature is a unique abiotic stress because the kinetics of all biochemical reactions and protein stability are affected by temperature. As such, temperature influences nearly all aspects of an ectothermic organism's physiology (Schulte 2015; Arcus et al. 2016). Therefore, adapting to a higher temperature may be much more difficult than adapting to a more specific environmental stress. For some anthropogenic stresses, such as antibiotics or herbicides, decades of research have revealed strong evolutionary adaptation to these stresses (Davies and Davies 2010; Powles and Yu 2010). However, genetic basis of adaptation to temperature is likely to be much more complex (Hochachka and Somero 2002).

The ability of an organism to tolerate different temperatures is often described by a thermal performance curve (Huey and Kingsolver 1989, 1993), which is the fitness or performance of

an organism as a function of temperature (Fig. 1A). These curves have been used to predict how organisms potentially respond to increased temperatures (Deutsch et al. 2008; Araújo et al. 2013; Sinclair et al. 2016). In general, thermal performance curves or reaction norms have been thought to evolve by either changes in elevation (Fig. 1B), left or right shifts in the curve that lead to changes in optimum temperature or temperature limits (Fig. 1C), or changes in curve shape (Fig. 1D).

Certain biochemical constraints may explain the characteristic shape changes of performance curves (Angilletta et al. 2003). For example, high enzyme stability could allow tolerating high temperatures with the expense of reduction of performance in cold temperatures resulting in a hot-cold trade-off. Synthesis of two enzymes with different optima could allow broader thermal tolerance but with an energetic expense of expressing two proteins, leading to reduction of performance at intermediate temperatures and producing a broad-narrow performance trade-off. Furthermore, the biochemical activation energy provided by higher temperatures can lead to

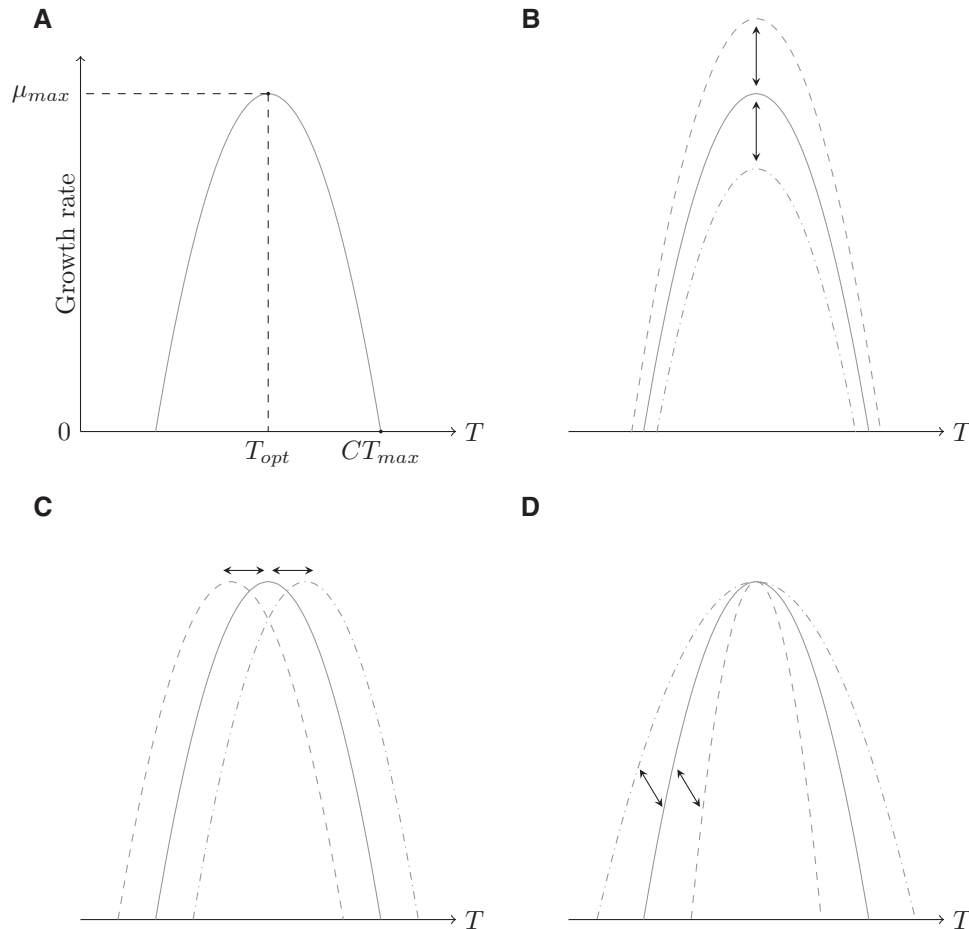


Figure 1. (A) An illustration of a hypothetical temperature performance curve. Temperature is on the horizontal axis and growth rate is on the vertical axis. T_{opt} shows the optimal temperature, where growth rate has its maximum value, μ_{max} . Temperature where growth rate reaches zero as temperature increases is denoted as CT_{max} . (B) Change in reaction norm elevation shifts the reaction norm on the vertical axis. (C) A horizontal shift. (D) Change in reaction norm shape.

thermodynamic effects: genotypes with higher optimal temperatures are expected to have higher performance (Hochachka and Somero 2002). Thermodynamic effect is also called the “hotter is better” hypothesis.

While several studies have tested how different species or populations differ in their thermal performance curves, or if evolution has been able to shape them (e.g., Krenek et al. 2011; Klepsatel et al. 2013; Ketola and Saarinen 2015; Ashrafi et al. 2018; Maclean et al. 2019), only a few studies have determined the evolutionary potential of thermal performance curves. In these studies, the genetic variance-covariance matrix (**G**-matrix) for thermal performance across several temperatures has been estimated, and how genetic variation is aligned with characteristic directions of reaction norm evolution has been determined (e.g., Izem and Kingsolver 2005; Stinchcombe et al. 2010; Latimer et al. 2015; Logan et al. 2020). This is essential to explore how freely thermal performance can evolve in different environments, and to quantify if thermal performance

evolution is bound to follow a certain evolutionary path or performance curve shape. Constraints on performance curve evolution will affect the ability of populations to respond to increasing temperatures, which is crucial, as studies suggest that plastic responses alone may not be enough for most species for dealing with coming temperature increases (Gunderson and Stillman 2015).

However, in the midst of multivariate genetics and the emphasis on finding genetic constraints, it should be remembered that evolutionary change in a particular direction is not necessarily completely prevented by moderate constraints. From quantitative genetic parameters one can only deduce which traits have the highest amount of variation, and what is the alignment of the **G**-matrix with respect to characteristic thermal performance curve shapes. However, unless genetic correlations are exactly -1 or 1 , or if selection occurs exactly to the direction of zero genetic variation, evolutionary change to a particular direction is not prohibited, only slowed down.

To explore constraints of thermal performance curve evolution, we are using the filamentous fungus *Neurospora crassa* as a model system to study the quantitative genetics of thermal performance curves. *Neurospora crassa* is a genetic model system that has been used extensively in different aspects of genetic research (Roche et al. 2014). Recently, some studies have started to explore quantitative variation in *N. crassa* (Ellison et al. 2011; Palma-Guerrero et al. 2013). This is despite *N. crassa* having excellent properties for the study of quantitative genetics: *N. crassa* can reproduce either asexually or sexually, so analysis of clones is possible for quantitative genetic experiments and controlled crosses can be made. Comparatively little is known about the ecology of *N. crassa*; it is a saprotrophic organism that decomposes dead plant matter, and it is particularly found on burned vegetation. Its geographic distribution is concentrated in mainly tropical and subtropical regions (Turner et al. 2001). Most strains have been collected from the Caribbean basin, southeastern United States, west Africa, and India (Turner et al. 2001), but the species also occurs in southern Europe (Jacobson et al. 2006).

Specifically, we asked the following questions: (1) Is there genetic variation in thermal performance curves in *N. crassa*? (2) Is variation in performance curves mainly for elevation, location, or shape? (3) Do constraints exist for performance curve evolution in the short term and what are these constraints?

To address how much genetic variation exists in temperature performance curves, we used a panel of strains of *N. crassa* that had previously been sampled from natural populations. We also crossed certain strains together to generate additional families. We measured the growth rates of these strains in different temperatures and combined these measurements into a thermal performance curve. We used a multivariate model to estimate the **G**-matrix of performance at different temperatures. We then used the empirical estimates of genetic variation in a quantitative genetic model to describe the short-term evolutionary potential of temperature performance curves of *N. crassa*.

Materials and Methods

Neurospora crassa STRAINS

We used a panel of strains originally obtained from the Fungal Genetics Stock Center (McCluskey et al. 2010). Our sample included natural strains collected from Louisiana (USA), the Caribbean, and Central America (Ellison et al. 2011; Palma-Guerrero et al. 2013), 113 natural strains in total. In addition we made crosses between some of the strains to obtain additional families to increase the genetic variation segregating among our lines. We crossed strains 10948 × 10886 to obtain family A ($n = 94$), 10932 × 1165 to obtain family B, ($n = 50$), 4498 × 8816 to obtain family C ($n = 50$), 3223 × 8845 to obtain family D ($n = 52$), and 10904 × 851 to obtain family G ($n = 69$).

Parents were chosen to have crosses within the Louisiana strains and between the Louisiana and Caribbean strains. In total, the panel contained 428 strains and based on genotypic data (Ellison et al. 2011; Palma-Guerrero et al. 2013) all strains represent unique genotypes. Table S1 contains a list and information about the strains. Strain numbering in family G runs up to 72 because strains G2, G9, and G51 grew very poorly and were excluded from the experiment.

PHENOTYPING

Standard laboratory methods were used to maintain *Neurospora* cultures (Davis and de Serres 1970). We measured growth rates using a tube method described in Kronholm et al. (2016) but instead of parafilm we used silicone plugs to cap the tubes. We measured the linear growth rate of each genotype in six different temperatures: 20°C, 25°C, 30°C, 35°C, 37.5°C, and 40°C. Temperatures were chosen based on the known reaction norm for strain 2489 (Kronholm et al. 2016). Three clonal replicates were measured for each genotype at each temperature. This gave a total of 7704 growth assays. In some assays the inoculation failed and the strain did not grow, or water droplets moved the inoculum along the pipette and linear growth rate could no longer be measured. There were 19 such assays and these were recorded as missing data, thus the number of growth assays in the final dataset was 7685. Strains were grown in two growth chambers (MTM-313 Plant Growth Chamber, HiPoint Corp., Taiwan) that contained three compartments, each with adjustable temperature. We rotated the temperatures among the different compartments between replicates, so that replicates of the same temperature were measured in different compartments, and monitored the temperature in the compartments with data loggers.

STATISTICAL ANALYSIS

All statistical analyses were performed with R 3.6.0 (R Core Team 2019). Bayesian models were implemented using the Stan language (Carpenter et al. 2017) which uses Hamiltonian Monte Carlo sampling. Hamiltonian Monte Carlo is much more efficient than traditional Markov chain Monte Carlo (MCMC) algorithms, such as Gibbs sampling, and can potentially accommodate very large number of parameters. An accessible introduction can be found in McElreath (2015). Stan was interfaced using the “brms” 2.9.0 R package (Bürkner 2018). MCMC convergence was monitored by trace plots and \hat{R} values. We considered parameter values to be different if their 95% highest posterior density (HPD) intervals did not overlap.

Thermodynamics of thermal performance curves

Theory predicts that if differences between hot and cold adapted genotypes are determined solely by an effect of temperature on metabolic rate, the thermodynamic effect or “hotter is better”

hypothesis, there should be a negative relationship between the logarithm of maximal growth rate, μ_{max} , and $1/(kT_{opt})$, where k is Boltzmann's constant and T_{opt} is the temperature (in K) at which maximal growth rate occurs (Savage et al. 2004). We examined whether differences between *N. crassa* genotypes could be solely explained by a thermodynamic effect. When $\ln(\mu_{max})$ is plotted against $1/(kT_{opt})$ the slope of a regression line is equal to negative activation energy, $-E$. The thermodynamic expectation for the slope is -0.6 because 0.6 eV is the average activation energy for biochemical reactions in the cell. This pattern generally holds across taxa adapted to different temperatures (Savage et al. 2004; Sørensen et al. 2018). Slopes > -0.6 have been interpreted as an indication of other physiological or biochemical reasons rather than a thermodynamic effect (Sørensen et al. 2018).

To calculate the optimum temperature for each genotype without using a specific model that may fit for some genotypes better than others, we fitted natural splines for each genotype. We extracted the maximum growth rate (μ_{max}) and optimum temperature (T_{opt}) from the spline fit. We then fit a model

$$\begin{aligned} \ln(y_i) &\sim N(\mu_i, \sigma) \\ \mu_i &= \alpha + \beta \times T_{opt,i} \\ \alpha, \beta &\sim N(0, 10) \\ \sigma &\sim \text{hC}(0, 2), \end{aligned} \tag{1}$$

where y_i is the i th maximum growth rate, α is the intercept, β is the slope, and $T_{opt,i}$ is the i th optimum temperature. We used weakly regularizing priors: a normal distribution for α and β , and a half-Cauchy distribution for σ with location 0 and scale 2. MCMC estimation was done using two chains, with a warmup of 1000 iterations, followed by 4000 iterations of sampling. For this analysis, we removed genotypes from the data that had very low maximal growth rates $\ln(\mu_{max}) < 1$, which is $\mu_{max} < 2.72$ mm/h, as they did not have the typical tolerance curve shape and were outliers. These genotypes typically grew very slowly and reaction norms were much flatter than typical ones, which leads to larger uncertainty in estimating the optimal temperature from the spline fits (Fig. S1A). Fourteen genotypes were removed, this left 414 genotypes for the analysis. However, because removing outlier observations can be considered subjective, we also applied robust regression with bisquare weights to the full data. Robust regression is a method that gives less weight to individual data points than ordinary regression and is less affected by outlier observations (Venables and Ripley 2002).

Estimation of genetic variance and covariance components

We were interested in estimating the genetic variance and covariance components for growth rates at different temperatures that

together describe different aspects of temperature performance curves. Because *Neurospora* can be propagated clonally, we can estimate genetic variance components using clonal analysis. Among genotype variance is an estimate of the genetic variance and within genotype variance is an estimate of the environmental variance (Lynch and Walsh 1998). We used a multivariate model to estimate genetic variance components at each temperature and the genetic correlations of all possible temperature pairs. The advantage of this approach is that we do not have to assume any particular shape for the temperature reaction norm. The multivariate model was

$$\begin{aligned} \mathbf{y}_i &\sim \text{MVN}(\boldsymbol{\mu}_i, \mathbf{E}) \\ \boldsymbol{\mu}_i &= \boldsymbol{\alpha} + \boldsymbol{\alpha}_{g[i]} \\ \boldsymbol{\alpha}_{g[i]} &\sim \text{MVN}(0, \mathbf{G}) \\ \mathbf{G} &= \mathbf{S}_G \mathbf{R}_G \mathbf{S}_G \\ \mathbf{E} &= \mathbf{S}_E \mathbf{R}_E \mathbf{S}_E, \end{aligned} \tag{2}$$

where $\boldsymbol{\alpha}$ is a vector of intercepts, $\boldsymbol{\alpha}_{g[i]}$ is a vector of genotypic effects, \mathbf{S}_G and \mathbf{S}_E are 6×6 diagonal matrices with genetic or environmental standard deviations on the diagonal, and \mathbf{R}_G and \mathbf{R}_E are matrices for genetic and environmental correlations, respectively. We used weakly informative priors by using the half location-scale version of Student's t -distribution with three degrees of freedom and 10 as the scale parameter. Thus, the prior for intercept effects was

$$\boldsymbol{\alpha} \sim \begin{pmatrix} \text{hT} & (3, & 2, & 10) \\ \text{hT} & (3, & 3, & 10) \\ \text{hT} & (3, & 4, & 10) \\ \text{hT} & (3, & 4, & 10) \\ \text{hT} & (3, & 4, & 10) \\ \text{hT} & (3, & 3, & 10) \end{pmatrix} \tag{3}$$

for growth rates from 20°C to 40°C. The prior for each standard deviation in the model was $\sigma \sim \text{hT}(3, 0, 10)$, and we used an lkj prior (McElreath 2015) for the correlation matrices: $\mathbf{R}_E, \mathbf{R}_G \sim \text{LKJ}(1)$. For MCMC estimation two chains were run with a warmup period of 1000 iterations, followed by 5000 iterations of sampling, with thinning set to 2. By inspecting MCMC traceplots (Fig. S2) and the diagnostic summary statistic \hat{R} , which was 1 for all parameters, we found no evidence of convergence problems.

Genetic correlations and temperature differences

We were also interested in how the genetic correlation of growth rates changes as temperatures are further apart. To examine how correlations change in a statistically rigorous manner, we calculated pairwise temperature differences for each estimated genetic correlation ($n = 15$), and fitted a Bayesian linear model with genetic correlation as the response, taking into account

Table 1. Genetic variances, covariances, correlations, and environmental variances for growth rates in different temperatures estimated from the multivariate model.

(°C)	20	25	30	35	37.5	40	σ_E^2
20	0.08 (0.07–0.09)	0.11 (0.1–0.13)	0.14 (0.12–0.16)	0.15 (0.13–0.18)	0.13 (0.11–0.15)	0.07 (0.05–0.09)	0.01 (0.01–0.01)
25	0.94 (0.93–0.96)	0.17 (0.15–0.19)	0.22 (0.19–0.25)	0.24 (0.21–0.28)	0.19 (0.16–0.22)	0.11 (0.09–0.14)	0.02 (0.02–0.02)
30	0.86 (0.83–0.89)	0.96 (0.94–0.97)	0.32 (0.28–0.36)	0.36 (0.31–0.41)	0.28 (0.23–0.32)	0.17 (0.13–0.21)	0.04 (0.03–0.04)
35	0.75 (0.7–0.79)	0.83 (0.79–0.86)	0.9 (0.88–0.92)	0.5 (0.43–0.57)	0.42 (0.36–0.48)	0.25 (0.2–0.3)	0.06 (0.05–0.07)
37.5	0.68 (0.62–0.73)	0.7 (0.65–0.75)	0.75 (0.7–0.8)	0.9 (0.88–0.92)	0.43 (0.37–0.49)	0.3 (0.25–0.35)	0.09 (0.08–0.1)
40	0.42 (0.33–0.51)	0.47 (0.39–0.56)	0.51 (0.43–0.59)	0.61 (0.54–0.68)	0.77 (0.72–0.82)	0.34 (0.29–0.4)	0.2 (0.18–0.22)

Note: The diagonal (in bold) contains genetic variances (σ_G^2), upper triangle contains genetic covariances ($\sigma_{G_x} \sigma_{G_y} r_{G_x,y}$), and lower triangle contains genetic correlations ($r_{G_x,y}$). The last column contains environmental variances (σ_E^2). Estimates are posterior means with 95% HPD intervals shown in parentheses.

Table 2. Comparison of different models for relationship between genetic correlations and temperature differences.

Model terms	LOOIC	diff (±SE)	Weight
$\alpha + \alpha_{40} \times c_i + \beta \times d_i$	−38.54	0 (0)	0.84
$\alpha + \alpha_{40} \times c_i + \beta \times d_i + \beta_{40} \times d_i \times c_i$	−35.18	3.36 (1.24)	0.16
$\alpha + \beta \times d_i + \beta_{40} \times d_i \times c_i$	−26.07	12.47 (5.49)	0
$\alpha + \beta \times d_i$	−14.12	24.42 (5.54)	0
α	−7.61	30.93 (6.34)	0

Note: Model terms correspond to different deterministic parts of the model in equation (4), α_{40} is an intercept effect for correlations involving 40°C and β_{40} is a slope effect for correlations involving 40°C. LOOIC, leave-one-out information criterion; SE, standard error.

the uncertainty in the estimated genetic correlations. This is a linear model with measurement error where uncertainty in the estimated genetic correlations is propagated to the intercept and slope estimates of the linear model; see McElreath (2015) for details. We compared models with or without slope effects for temperature and whether genetic correlations involving growth rate at 40°C had a different intercept or slope (Table 2). We used the leave-one-out cross-validation method for model comparisons, implemented in the “loo” R package (Vehtari et al. 2017). The models were compared using the leave-one-out information criterion; smaller values indicate greater support for a model. The final model was

$$x_{est,i} \sim N(\mu_i, \sigma) \tag{4}$$

$$\mu_i = \alpha + \alpha_{40} \times c_i + \beta \times d_i$$

$$x_{obs,i} \sim N(x_{est,i}, x_{sd,i})$$

$$\alpha, \alpha_{40}, \beta \sim N(0, 10)$$

$$\sigma \sim \text{hC}(0, 2),$$

where $x_{obs,i}$ is the median of i th observed genetic correlation, $x_{sd,i}$ is the observed standard deviation of i th genetic correlation, $x_{est,i}$ is the estimated genetic correlation for i th observation, α is the intercept, α_{40} is the intercept effect when one of the temperatures is 40°C, c_i is an indicator variable whether one of the temperatures is 40°C, β is the slope effect, and d_i is the temperature difference for the i th observation. MCMC estimation

was done using two chains, with a warmup of 1000 iterations, followed by 4000 iterations of sampling.

Quantitative genetics

We estimated broad-sense heritability, the proportion of genetic variance of the total variance, for each temperature as

$$H^2 = \frac{\sigma_G^2}{\sigma_G^2 + \sigma_E^2}, \tag{5}$$

where σ_G^2 is the genetic variance component and σ_E^2 the environmental variance component. Because *Neurospora* is haploid, the dominance variance component is not defined. Genetic variance in haploids is composed of

$$\sigma_G^2 = \sigma_A^2 + \sigma_{AA}^2 + \sigma_{AAA}^2 + \dots, \tag{6}$$

where σ_A^2 is the additive variance and σ_{AA}^2 is the additive × additive epistatic variance, σ_{AAA}^2 is the additive × additive × additive variance, and so on (Lynch and Walsh 1998). With our experimental design we cannot estimate the epistatic variance terms, as is the case with many other common quantitative genetic designs, and going further we assumed that epistatic variances were small and were ignored. This seems like a strong assumption, but there is some justification for doing so: even if there is plenty of epistasis at the level of gene action, this is not necessarily translated into epistatic variance (Hill et al. 2008; Mäki-Tanila and Hill 2014). Empirical data also suggest that most genetic variation is additive (Hill et al. 2008). The genetic covariance of traits

1 and 2 is $\text{cov}_{G_{1,2}} = \sigma_{G_1}\sigma_{G_2}r_{G_{1,2}}$, where $r_{G_{1,2}}$ is the correlation of the standard deviations or the genetic correlation. Thus, the genetic correlation for traits 1 and 2 can be defined as

$$r_{G_{1,2}} = \frac{\text{cov}_{G_{1,2}}}{\sigma_{G_1}\sigma_{G_2}}. \quad (7)$$

In addition to heritabilities, we used coefficients of variation to compare genetic and environmental variances. Heritability can be influenced by changes in either genetic or environmental variance, and genetic variance by itself is not a unitless variable (Houle 1992). The genetic coefficient of variation was

$$CV_G = 100 \times \frac{\sigma_G}{\bar{z}}, \quad (8)$$

where \bar{z} is the mean phenotype. Accordingly, the environmental coefficient of variation was $CV_E = 100\sigma_E/\bar{z}$.

We obtained the **G**-matrix to describe how the growth rates at different temperatures were correlated and to be able to calculate multivariate responses to selection for thermal performance curves. This matrix contains genetic variance components on the diagonal and covariance components on off-diagonals, so for n traits **G** is an $n \times n$ matrix:

$$\mathbf{G} = \begin{pmatrix} \sigma_{G_1}^2 & \sigma_{G_1}\sigma_{G_2}r_{G_{1,2}} & \cdots & \sigma_{G_1}\sigma_{G_n}r_{G_{1,n}} \\ \sigma_{G_1}\sigma_{G_2}r_{G_{1,2}} & \sigma_{G_2}^2 & \cdots & \sigma_{G_2}\sigma_{G_n}r_{G_{2,n}} \\ \vdots & \vdots & \ddots & \vdots \\ \sigma_{G_1}\sigma_{G_n}r_{G_{1,n}} & \sigma_{G_2}\sigma_{G_n}r_{G_{2,n}} & \cdots & \sigma_{G_n}^2 \end{pmatrix}. \quad (9)$$

For environmental variance, it is possible to construct an analogous **E**-matrix that is the environmental variance-covariance matrix.

We performed eigen decomposition of the **G**-matrix to gain insight into genetic constraints of reaction norm evolution. The eigenvector corresponding to the leading eigenvalue, or the first principle component, gives the direction of multivariate evolution with the least genetic resistance (Schluter 1996). We obtained these components by principle component analysis of the **G**-matrix. To assess uncertainty in the eigen decomposition we constructed a **G**-matrix for each posterior sample and performed decomposition for each **G**-matrix to obtain posterior distributions for how much variance the different components explained and for the component loadings. Obtaining interval estimates for the loadings this way is valid only if the order of eigenvectors stays consistent between the samples, and we could confirm this for components one and two.

To assess evolvability and constraint across the different growth rates we used the approach of Hansen and Houle (2008). Assuming there is a directional selection gradient β in multivariate space, they define evolvability as the length of the response to selection in the direction of β , this is the same as projection of

response to selection on β (Hansen and Houle 2008). Evolvability was calculated as

$$e(\beta) = \frac{\beta^T \mathbf{G} \beta}{|\beta|^2}. \quad (10)$$

Furthermore they define conditional evolvability as the response to selection in the direction of β , assuming that there is stabilizing selection around the direction of β and the population cannot deviate from this direction. For conditional evolvability we first calculated the unit vector of β as

$$\hat{\beta} = \frac{\beta}{|\beta|}$$

and conditional evolvability is then

$$c(\hat{\beta}) = (\hat{\beta} \mathbf{G}^{-1} \hat{\beta})^{-1}. \quad (11)$$

To assess whether evolvability along a certain selection gradient is particularly high or low it is possible to calculate average evolvabilities over random selection gradients in phenotypic space. Hansen and Houle (2008) derived analytical and approximate solutions for average evolvability and average conditional evolvability and we calculated these following their approach. Evolvabilities for single traits are just the genetic variances of those traits. Conditional evolvability for a single trait can be measured with respect to other traits. Conditional evolvability for trait i is $c_i = 1/[\mathbf{G}^{-1}]_{ii}$, where $[\mathbf{G}]_{ii}$ is the i th diagonal element of the **G**-matrix. Trait autonomy, the proportion of evolvability that remains after conditioning for the other traits, is calculated as $a_i = ([\mathbf{G}^{-1}]_{ii}[\mathbf{G}]_{ii})^{-1}$ (Hansen and Houle 2008). As there are scale differences in the growth rates at different temperatures, we calculated conditional evolvabilities for both on the original scale and on mean standardized scale. The **G**-matrix can be mean standardized by dividing i j th element by the product of the means of traits i and j . $\mathbf{G}_\mu = \mathbf{G} \oslash (\bar{\mathbf{z}}\bar{\mathbf{z}}^T)$, where $\bar{\mathbf{z}}$ is a vector of trait means and \oslash symbol for element-wise division. The mean standardized selection gradient was calculated as $\beta_\mu = \bar{\mathbf{z}} \odot \beta$, where \odot is element-wise multiplication. Interval estimates for these statistics were obtained by calculating them for each posterior sample.

Quantitative genetic model for the evolution of performance curves

To examine how thermal performance curves of *N. crassa* can evolve, we used a quantitative genetic model with the empirically estimated **G**-matrix. Response to selection can be calculated using the multivariate breeder's equation

$$\mathbf{R} = \mathbf{G}\mathbf{P}^{-1}\mathbf{S}, \quad (12)$$

where **S** is a vector of selection differentials for each temperature, **G** and **P** are the genetic and phenotypic variance-covariance matrices, respectively, and **R** is the response to selection. Response

to selection can also be expressed in terms of the selection gradient, β , as

$$\mathbf{R} = \mathbf{G}\beta, \quad (13)$$

where $\beta = \mathbf{P}^{-1}\mathbf{S}$. The biological interpretation of selection differential and selection gradient are different, as a selection differential of 0 for a given trait does not imply selective neutrality but rather stabilizing selection, whereas a selection gradient of 0 for a trait implies that the trait is selectively neutral. See Figure S3 for an illustration of the differences between these concepts. When we asked how evolution would proceed in a particular direction, we simulated the response to selection using selection gradient (eq. 13). And when we asked whether selection could generate a particular phenotype we simulated the response to selection using selection differentials (eq. 12). Our goal is not to predict the evolution of tolerance curves in nature, as the real selection gradients are unknown and the assumption that \mathbf{G} remains constant is likely violated in real populations. Indeed, there are considerable difficulties in predicting the response to selection in nature (Morrissey et al. 2010). Instead, our goal is to illustrate how thermal performance curves could evolve in a population with a similar \mathbf{G} as estimated empirically here.

The phenotypic matrix was calculated from $\mathbf{P} = \mathbf{G} + \mathbf{E}$. The environmental variance-covariance matrix \mathbf{E} , which uses environmental standard deviations and their correlations analogous to equation (9), was obtained from the same model fit as \mathbf{G} . As there is uncertainty in our estimates of \mathbf{G} and \mathbf{E} we incorporated this uncertainty in the selection responses by sampling 1000 \mathbf{G} and \mathbf{E} matrices from the posterior distributions of genetic and environmental standard deviations and calculating a response to selection for each sample. We calculated responses to selection after 1, 3, and 5 generations of selection, assuming that the selection differentials, \mathbf{G} , and \mathbf{E} matrices stay the same. We always normalized the sum of absolute values of selection differentials or gradients across all temperatures for different selection regimes. First, we used selection gradients that corresponded to the first two eigenvectors of the \mathbf{G} -matrix. The summed absolute values of selection gradients or selection differentials across all temperatures were normalized to be 0.6 mm/h. We estimated evolvability and conditional evolvability along these gradients as explained above. Then we used different selection regimes to examine how we could change the performance curve elevation, optimum, or shape (Fig. 1). We used six different vectors of \mathbf{S} : $\mathbf{S}_1 = \{0.1, 0.1, 0.1, 0.1, 0.1, 0.1\}$ and $\mathbf{S}_2 = \{-0.1, -0.1, -0.1, -0.1, -0.1, -0.1\}$, which correspond to selection on elevation change; $\mathbf{S}_3 = \{0, 0.1, 0.1, -0.2, -0.2, 0\}$ and $\mathbf{S}_4 = \{0, -0.05, -0.05, -0.1, 0.2, 0.2\}$, which correspond to a shift in optimum temperature; $\mathbf{S}_5 = \{0.1, 0.2, 0, 0, 0.1, 0.2\}$ and $\mathbf{S}_6 = \{0, -0.1, -0.25, 0.05, -0.1, -0.1\}$, which correspond

to change in reaction norm shape. The selection differentials were chosen so that they would produce the desired phenotypic change, choice of numerical values was otherwise arbitrary. For evolvability calculations, we calculated realized selection gradients based on these selection differentials as $\beta = \mathbf{P}^{-1}\mathbf{S}$.

Results

GROWTH OF *Neurospora* AT DIFFERENT TEMPERATURES

Temperature had a large effect on growth, at 20°C growth rate was between 2 and 2.5 mm/h (mean 2.17 and 95% HPD interval 2.15–2.20) for most strains, and as temperature increased up to 35°C growth rates rose to between 3 and 5 mm/h (mean 4.15% and 95% HPD interval 4.08–4.22) for most strains (Fig. 2A). This represents an increase of 91% in mean growth rate. For many strains growth rate peaked at 35°C and then decreased as temperature was increased (Fig. 2A), at 40°C mean growth rate was 2.35 (2.29–2.41 95% HPD interval) mm/h. The performance curves of *N. crassa* exhibited a typical performance curve form: with an optimum temperature and decrease in growth rate in other temperatures, and performance declined faster in temperatures warmer than the optimum (Sinclair et al. 2016). Few genotypes grew very slowly and had unusual tolerance curve shapes (Fig. 2A), possibly reflecting that these genotypes were poorly suited to lab conditions, due to specific nutritional requirements, for example.

THERMODYNAMICS OF THERMAL PERFORMANCE CURVES

We examined whether differences between genotypes could be explained by a thermodynamic effect, that is, does the maximum growth rate increase with optimum temperature. We obtained μ_{max} and T_{opt} from the natural spline fits and plotted $\ln(\mu_{max})$ against $1/(kT_{opt})$ (Fig. 2B). For the bulk of the genotype data, the estimated slope was -0.16 (95% HPD from -0.22 to -0.10), which corresponds to activation energy of 0.16 eV. This was lower than the theoretical expectation of 0.6 eV. Moreover, there was substantial amount of variation around the regression line (Fig. 2B); optimum temperature explains only a small proportion of the observed variation. This indicates that while a small thermodynamic effect exists, most variation within *N. crassa* is due to other physiological and biochemical causes. As this result was obtained in an analysis where we removed genotypes that had atypical reaction norms (Fig. S1A), we also fitted a robust regression to the full data (Fig. S1B) and obtained a slope of -0.17 , which is very close to our original estimate of -0.16 . While fitting an ordinary regression to the full data gives a more negative slope (-0.34), the few atypical observations have high leverage in the model. As results of robust regression and

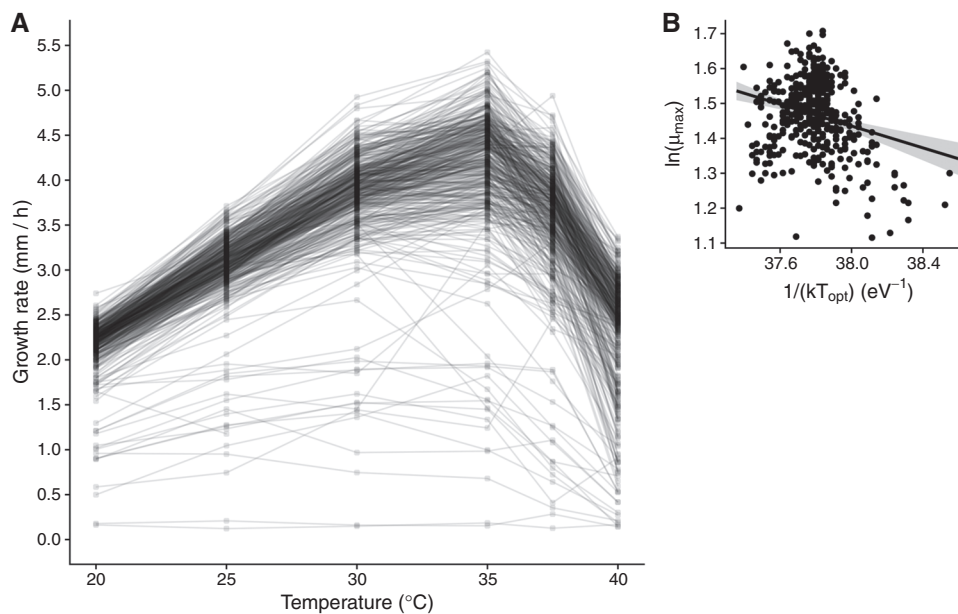


Figure 2. (A) Phenotypic means for each genotype. (B) Logarithm of maximum growth rate, μ_{max} , plotted against inverse of kT_{opt} , where k is the Boltzmann's constant and T_{opt} the temperature where maximal growth rate occurs. The slope gives an estimate of negative activation energy $-E$.

removing outliers agree, it seems that removing the outliers is quite reasonable in this case.

QUANTITATIVE GENETICS

To analyze the data without forcing the tolerance curves to fit any predetermined shape, or underlying latent structures as in Izem and Kingsolver (2005), we fit a multivariate model to the data where growth at each temperature was modeled as potentially correlated with growth at other temperatures. We obtained the **G**-matrix from the multivariate model fit (eq. 2). There was genetic variation for growth in all temperatures and all genetic covariances and correlations were positive (Table 1).

By plotting the model means and genetic correlations it appeared that genetic correlation between adjacent temperatures was generally high, and decreased as temperatures were further apart and correlations involving 40°C also seemed lower (Fig. 3A). We tested this idea formally and fitted a model of genetic correlations and temperature differences. We compared the different models, and the best model had different intercepts for correlations involving 40°C and for correlations not involving 40°C, and identical slopes for these two groups (Table 2). A model with both different slopes and different intercepts had marginal weight in the model comparison but the β_{40} parameter had an estimate overlapping with zero, so this model gave the same results as the simpler model and thus we report results only from the different intercepts model. The model confirmed our observation that the genetic correlation between any two temperatures was indeed lower if one of those temperatures was

40°C (Fig. 3B), the intercept effect α_{40} had an estimate of -0.24 (with a 95% HPD interval from -0.31 to -0.17). The genetic correlation of growth rates in two temperatures decreased by 0.02 (0.02–0.01 95% HPD interval) units as temperature difference increased by 1°C. This result suggested that variation in different genes contributes to genetic variation for growth at 40°C than in lower temperatures.

Most of the variation observed in growth rates was due to genetic variation present among the strains. Heritabilities for growth at different temperatures were high, around 0.89 for temperatures from 20°C to 35°C (Fig. 3C). As temperature increased further heritability dropped to 0.63 at 40°C (Fig. 3C). However, this lower heritability was not due to decreased genetic variation but to increased environmental variance at 37.5°C and 40°C (Table 1). Therefore there was substantial genetic variation for growth rate at 40°C but environmental variation increased as well; looking at heritability alone would have been misleading in this case. Furthermore, as trait means differ across the different temperatures looking at genetic variances alone would have suggested that 35°C has the most genetic variance (Table 1), but this would have been also misleading as the coefficient of genetic variation reveals that growth at 40°C has the most genetic variation followed by the other temperatures in decreasing order (Fig. 3D). The same was true for coefficient of environmental variation (Fig. 3D).

Eigen decomposition of the **G**-matrix can reveal what are the main axes along which correlated traits most readily evolve. We used principle component analysis to decompose

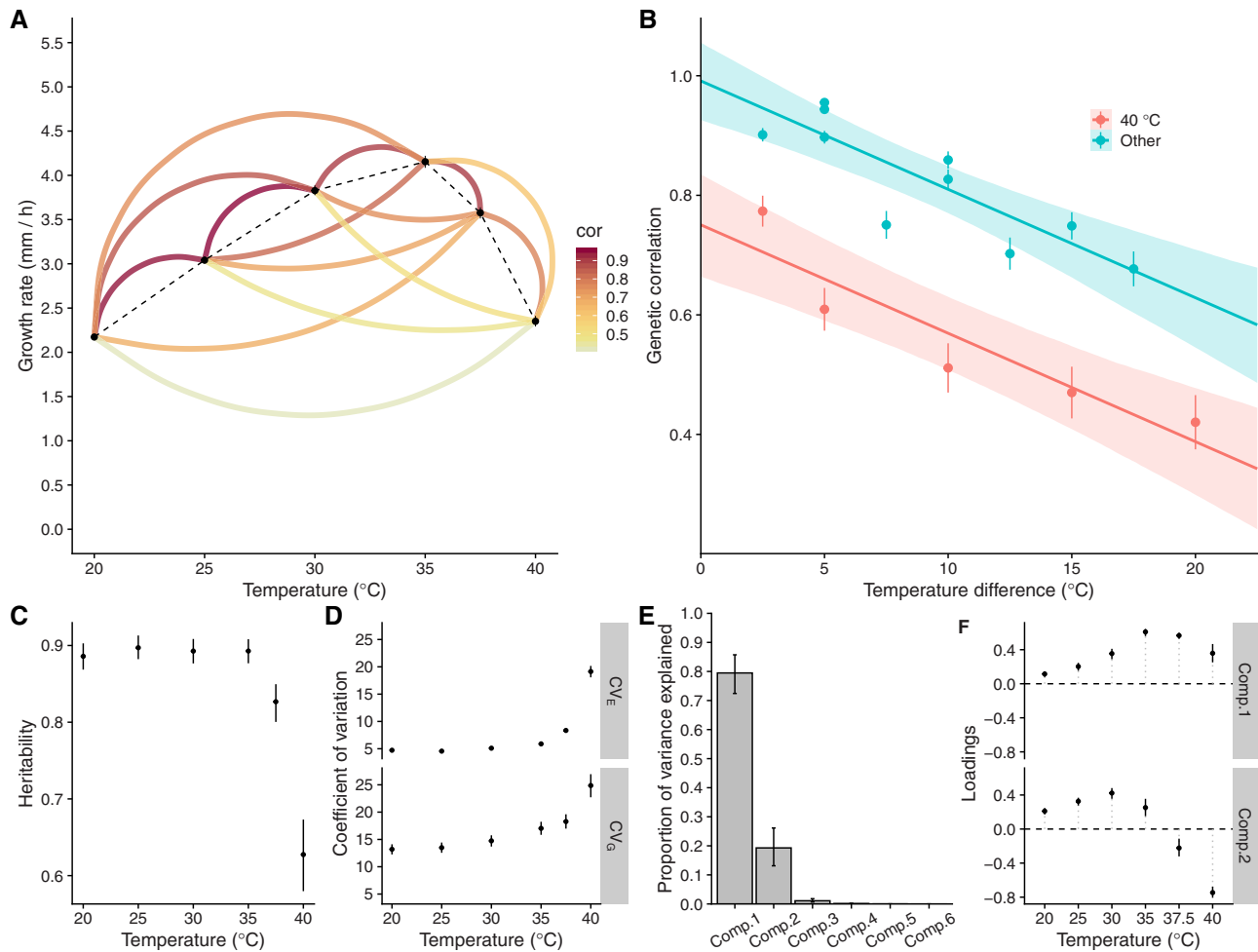


Figure 3. (A) Model means and genetic correlations for each temperature. Arcs connect each pair of temperatures and arc color corresponds to the strength of their genetic correlation. (B) Genetic correlations against temperature differences. Line is the mean slope of the model and envelope the 95% HPD interval for the slope. (C) Heritabilities of growth rate at each temperature, means and 95% HPD intervals. (D) Coefficients of genetic and environmental variation for each temperature, means and 95% HPD intervals. Note that points obscure small error bars. (E) Principle component analysis of the G-matrix: proportions of variance explained by the different components. Error bars are 95% HPD intervals. (F) Loadings of components 1 and 2 for each temperature. Error bars are 95% HPD intervals.

the **G**-matrix. The first two principle components explained most of the variance with the first component explaining 79.5% (72.4–86.0%) and the second component 19.3% (13.1–26.6%) of the variance (Fig. 3E). The rest of the components explained the remaining 1.2% of the variance, but the sizes of their corresponding eigenvalues were so small that this 1.2% is unlikely to have any biological meaning. Moreover, the interval estimates for the loadings of components 1 and 2 were consistent with no sign changes (Fig. 3F), but this was not the case for rest of the components, indicating that loadings for the rest of the components are very uncertain. All the loadings of the first principle component were positive (Fig. 3F), indicating that most variation in tolerance curves is mainly for elevation. The second component suggested that growth rate at 40°C and to a lesser extent at 37.5°C are more independent from the other

temperatures, even though the genetic correlation between 40°C and the other temperatures were positive (Table 1).

When looking at trait-specific evolvabilities, we also observed that growth rate at 40°C had the highest conditional evolvability and the highest autonomy (Table 3). This indicates that out of all of the growth rates, growth rate at 40°C can evolve by itself most easily. The rest of the traits had very low autonomies reflecting their high genetic correlations (Tables 1 and 3).

EVOLUTION OF PERFORMANCE CURVES

To examine how a performance curve of a population that has the same **G**-matrix as estimated here could evolve, we performed simulations with a quantitative genetic model of performance curve evolution. First we asked how performance curves responded to selection if selection were to operate in the same

Table 3. Conditional evolvabilities (c_i) and autonomies (a_i) for growth rates at different temperatures, values are posterior medians and 95% HPD interval is shown in parentheses.

(°C)	No standardization	Mean standardized	a_i
	c_i	c_i	
20	0.006 (0.004–0.008)	0.0013 (0.0008–0.0018)	0.07 (0.05–0.10)
25	0.004 (0.003–0.006)	0.0005 (0.0003–0.0007)	0.03 (0.02–0.04)
30	0.012 (0.008–0.017)	0.0008 (0.0006–0.0011)	0.04 (0.03–0.05)
35	0.029 (0.021–0.038)	0.0017 (0.0012–0.0022)	0.06 (0.04–0.08)
37.5	0.033 (0.022–0.045)	0.0026 (0.0017–0.0035)	0.08 (0.05–0.11)
40	0.106 (0.075–0.139)	0.0190 (0.0134–0.0249)	0.31 (0.22–0.40)

Note: For conditional evolvability values for both without standardization and with mean standardized G-matrices are shown. Values for trait-specific autonomy are the same with and without standardization.

direction as the two first observed loadings of the G-matrix eigen decomposition (Fig. 3F). We normalized the summed absolute values of selection gradients across all temperatures to be 0.6 mm/h and their relative weights to be proportional to the loadings of each principle component. Theoretical prediction is that when β is in the same direction as the first component, evolvability should be the greatest (Schluter 1996). Indeed, this is what we observed, as the response to selection was also greatest in this direction (Fig. 4). Moreover, evolvability and conditional evolvability greatly surpassed the average evolvability across the entire phenotypic space (Fig. 4D). When the selection gradient pointed to the direction of the second component, unconditional evolvability was no longer larger than expected, while conditional evolvability still remained larger than average (Fig. 4D).

Next we examined responses to different selection differentials with the idea that we want to know whether particular phenotypic change in the performance curve was possible, whatever the selection gradient implied by the selection differentials. For instance, when we simulated selection for increased growth at a single temperature this led to positive correlated responses in other temperatures if the other traits were neutral, as in the case when selection gradient is zero for a given trait. However, when there was selection for increased growth at a single temperature and to maintain the original phenotype at the other temperatures there were also correlated responses but these were less uniform (Fig. S3). Accordingly, selection at a single temperature often leads to correlated responses in nearby temperatures (Fig. S4). Selection at multiple temperatures led to stronger responses to selection and correlated responses (Figs. S5 and S6). For instance, selection at 25 and 30°C also increased growth rate at 20°C (Fig. S5). When selection happened at multiple temperatures, response could be larger in certain temperature than if selection happened for that temperature alone. For example, if there was selection for higher growth at 20°C, 25°C, and 30°C, response to selection was greater than if there was selection for higher growth only at 20°C (Fig. S4 and S6). With selection differential of 0.2 only

at 20°C, response to selection after five generations was 2.80 (2.75–2.84, 95% HPD), whereas if selection differential was 0.2 at 20, 25, and 30°C, response to selection after five generations of selection was 3.01 (2.98–3.04, 95% HPD). Thus, it was not possible to change a certain temperature completely independently of the others, but often extreme temperatures could be changed without affecting the growth at the other extreme.

We then asked is it possible to create similar evolutionary responses in performance curves as shown in Figure 1. We were able to find a set of selection differentials that were able to generate changes in elevation, horizontal shift, or shape (Fig. 5). This shows that despite strong genetic correlations it is possible for the performance curves to evolve in almost any manner if selection favors such a performance curve. However, selection regimes involving horizontal shifts require selection for increased growth rate in some temperatures and decreased growth rate in others (Fig. 5). Evolvabilities and conditional evolvabilities were highest for elevation changes. For optimum shifts and shape changes conditional evolvabilities were lower than the average conditional evolvability over all phenotypic space (Fig. 5C). This indicates that elevation changes are less constrained than changes in optimum temperature or performance curve shape.

Discussion

We have shown that there is substantial genetic variation in thermal performance curves of *N. crassa*. Most of this variation is in performance curve elevation and there is very little evidence of strong trade-offs. Genetic variation in growth is strongly correlated among nearby temperatures but there is a threshold before or at 40°C after which this correlation drops, indicating that physiological processes at 40°C are different from those at lower temperatures. Such thresholds are common in many organisms, including *Drosophila* where different expression profiles were observed in cold, moderate, and hot temperatures (Colinet et al. 2013).

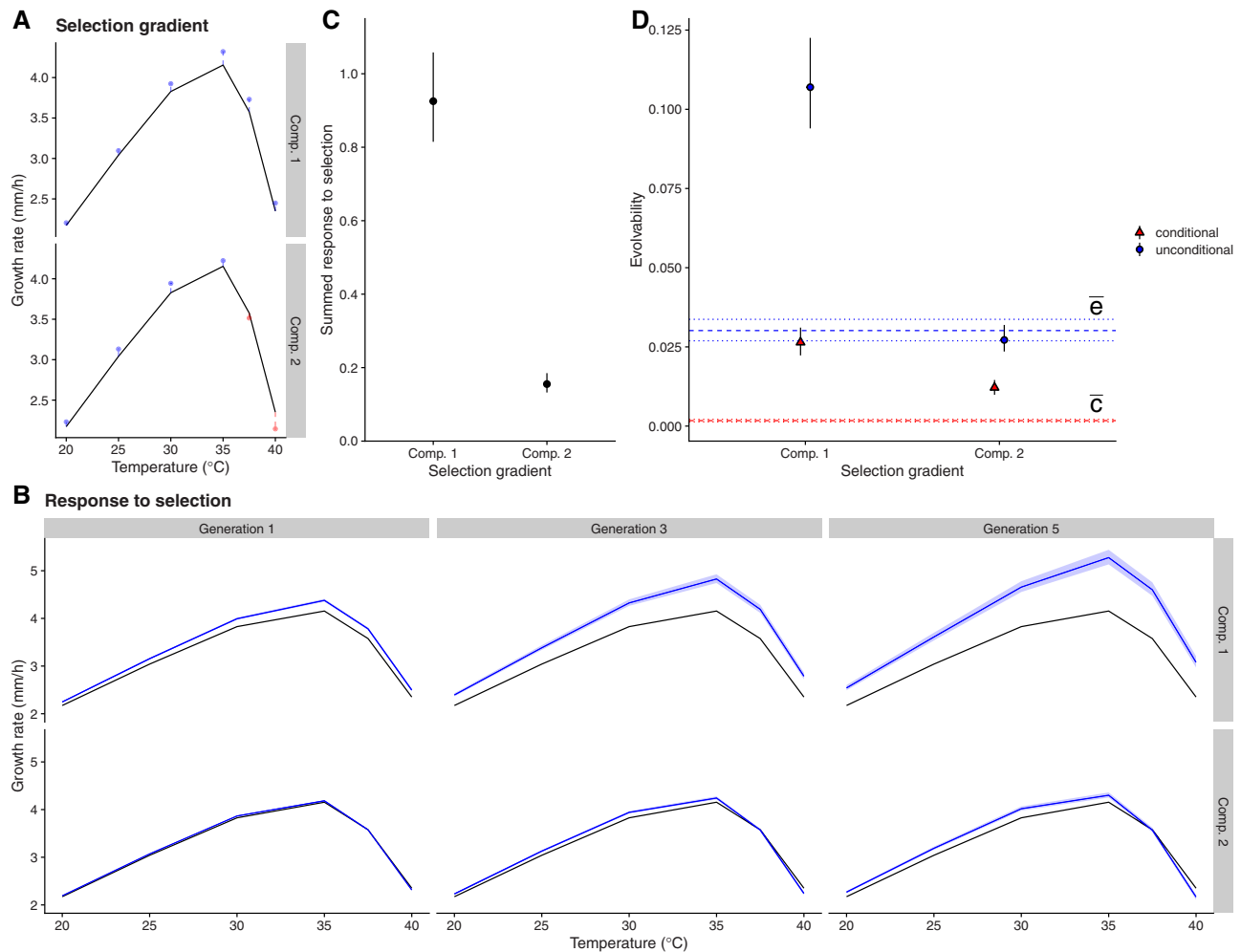


Figure 4. Simulated responses to selection using selection gradients, β . (A) Selection gradients correspond to the loadings of the first two components of the G-matrix eigen decomposition. Black line is the mean empirical performance curve and dots represent values of selection gradient for each temperature. Blue dots represent selection for increased growth and red dots for decreased growth. (B) Simulated responses to selection, black line is the empirical mean and blue lines are the simulated performance curves after selection. Shaded regions contain 95% of the simulations. Note that variability due to uncertainty in the G-matrix is not visible for many of the simulations. Columns show selection responses after 1, 3, or 5 generations of selection and rows show results for different selection regimes. (C) Summed absolute values for response to selection in a single generation for the two gradients. (D) Medians and 95% intervals for mean standardized evolvabilities for the two gradients, blue horizontal lines (e) show the average unconditional evolvability across random selection gradients and red horizontal lines (c) show the average conditional evolvability, dotted lines show the 95% HPD interval.

In many ways, variation in performance curves of *N. crassa* are quite typical for many ectotherms that have been studied (Sinclair et al. 2016). Most genetic variation in *N. crassa* is variation in performance curve elevation, which contrasts with previous studies in other species that have found most variation to be for reaction norm shapes (Izem and Kingsolver 2005; Logan et al. 2020). Yet variation in performance curve elevation is commonly found. A review of thermal performance curves in insects found that elevation shifts were the most common type of change along environmental gradients (Tüzün and Stoks 2018), see also Scheiner (1993). We also observed quite substantial heritabilities overall, and while comparisons between animals

and fungi should be treated with caution, other studies have observed much lower heritabilities (e.g., Logan et al. 2018; Castañeda et al. 2019; Martins et al. 2019).

Genetic variation in performance curve elevation could reflect differences in genetic condition of individuals, that is, the number of deleterious mutations different individuals carry, rather than temperature-specific adaptation. A good estimate of effective population size is not available at the moment, so some uncertainty remains. However, deleterious mutations seem an unlikely explanation as *N. crassa* is haploid, so deleterious mutations are immediately exposed to selection and would be removed, as in nature there is plenty of sexual reproduction as

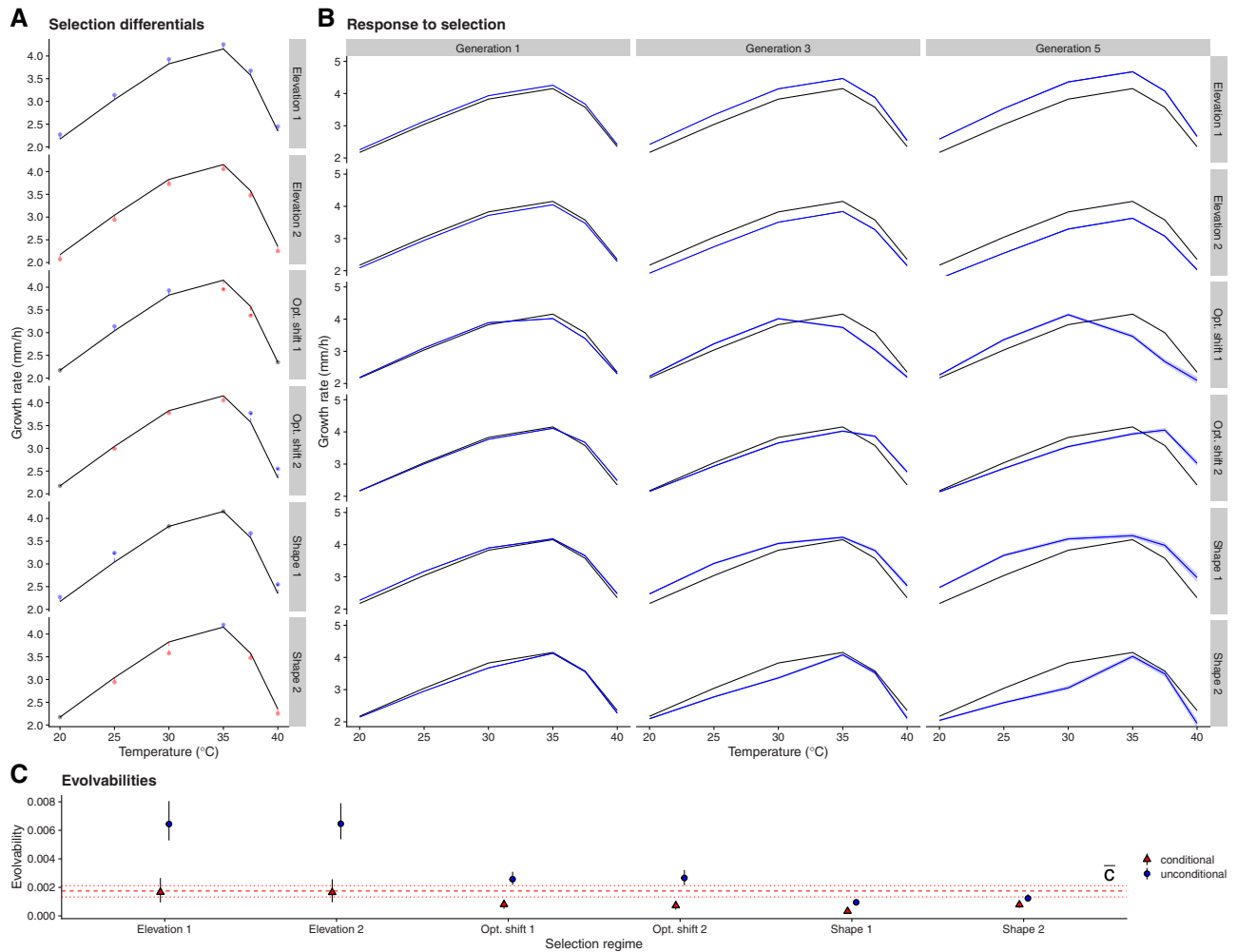


Figure 5. Simulated responses to selection using selection differentials, *S*. (A) Selection differentials for each selection regime. Black line is the mean empirical performance curve and dots represent values of selection differentials for each temperature. Blue dots represent selection for increased growth, red for decreased growth, and black dots indicate stabilizing selection at this temperature. Selection regime 1 selects for increased elevation, regime 2 selects for decreased elevation, regime 3 selects for lower optimum temperature, regime 4 selects for higher optimum, regime 5 selects for broader shape, and regime 6 selects for narrower shape. (B) Simulated responses to selection. (C) Evolvability and conditional evolvability for each of the selection gradients implied by the selection differentials. Red horizontal lines show the average conditional evolvability (\bar{c}) across the entire phenotypic space. Average evolvability is higher than the y-axis scale and is not shown.

indicated by rapid decay of linkage disequilibrium in the population genetic data (Ellison et al. 2011; Palma-Guerrero et al. 2013). Another possibility, that is not temperature-specific adaptation, is that genetic differences between the strains in how well they are able to grow in lab conditions are thermodynamically amplified, as increasing temperature also increases metabolic rate (Schulte 2015). However, our estimates of activation energy were much lower than the thermodynamic expectation, and contrast with previous studies that have found much stronger relationship between growth rate and optimum temperatures (Savage et al. 2004; Knies et al. 2009; Sørensen et al. 2018). While we cannot exclude that some of the differences were due to the thermodynamic effect, this cannot be the whole explanation as there were

clear genotype by environment interactions indicated by genetic correlations across environments that were less than one. There have to be alleles segregating in the population that have different effects in different temperatures. Particularly, genetic variation after the optimum of the thermal performance curve has been reached cannot be accounted by thermodynamic effects (Schulte 2015).

There was no indication of strong trade-offs between temperatures, and certainly not the kind of trade-offs that have been assumed in many models of tolerance curve or reaction norm evolution in general (Angilletta et al. 2003). The absence of any trade-offs suggests that theoretical models of reaction norm evolution that assume trade-offs should be treated with caution.

It further poses a question: if growth rate is closely linked to fitness, and if there are no trade-offs, why there is genetic variation in growth? It seems reasonable that mycelial growth rate should be a fitness component in filamentous fungi. In a previous study, no trade-off was detected between mycelial growth rate and spore production (Anderson et al. 2018). However, there is some evidence that strains that have higher growth rates also have higher competitive fitness (Kronholm et al. 2020). It may be that there is a trade-off between growth rate and some other trait that we have not measured, for example, Ketola et al. (2013) found a trade-off between bacterial virulence and growth in high temperatures. Alternatively, the evolution of performance curves may be limited by the environments, and thus the selection pressures, the strains encounter rather than genetic trade-offs (Whitlock 1996; Kassen 2002). If there is no selection at a particular temperature, then variation at those temperatures may be neutral. The evidence for trade-offs and cost of plasticity for temperatures has been mixed; some studies have observed trade-offs (Knies et al. 2006; Romero-Olivares et al. 2015; Le Vinh Thuy et al. 2016), while others have observed that adapting to one temperature did not limit plasticity (Manenti et al. 2015; Fragata et al. 2016), most genetic variation has been observed for overall performance (Klepsatel et al. 2013; Latimer et al. 2015), or that adaptation was largely temperature specific with no apparent trade-offs (Bennett et al. 1992).

Genetic correlations between growth rates at nearby temperatures were strong, which is to be expected, as a difference of a few °C is likely to be a very similar physiological environment for an organism. However, growth rate at 40 °C had a lower genetic correlation to growth rates at other temperatures. This suggests that at 40 °C there was some physiological process activated, which has genetic variation, but that was not active or was at much lower level of activity in lower temperatures. The most obvious candidate for such a process is the heat-shock response (Piper 1993; Feder and Hofmann 1999; Sørensen et al. 2003). Previously, the heat-shock response of *N. crassa* has been studied at 42 °C or higher (Plesofsky-Vig and Brambl 1985; Guy et al. 1986; Mohsenzadeh et al. 1998) but it probably occurs already at lower temperatures, as we observed significant slowdown of growth at 40 °C. The canonical heat-shock proteins are important for the physiological heat-shock response, but there can be additional mechanisms involved: there is evidence that the sugar trehalose plays some role in *N. crassa* heat-shock response (Bonini et al. 1995). Furthermore, changes in cell membrane composition are involved in temperature acclimation and the proportion of highly unsaturated fats increases in low temperatures (Martin et al. 1981). These responses have been observed in yeasts as well (Glatz et al. 2015). It is likely that there is genetic variation in the heat-shock response induction threshold or in the magnitude of heat-shock response, and this physiological varia-

tion can explain why the genetic correlation across temperatures is lower when 40 °C is involved. Further investigation into variation of heat-shock responses at the physiological level seems warranted.

Conclusions

At the species level, populations of *N. crassa* contain plenty of genetic variation for growth at different temperatures, and may be able to respond to increasing temperatures and thermal fluctuations via genetic adaptation mainly by increasing overall performance. An experimental evolution study with a related species, *N. discreta*, also demonstrated adaptation to higher temperature (Romero-Olivares et al. 2015). Previous studies have suggested that warming may pose the greatest risk to tropical animal species, as they live already close to their thermal maxima (Deutsch et al. 2008), but *N. crassa* may be different in this respect as high temperatures in the Caribbean average around 30 °C. Whether this is true for all fungi or if *N. crassa* is a special case remains to be investigated.

We did not observe any inherent genetic trade-off between hotter and colder temperatures, which is in contrast to common theoretical assumptions. Thermal performance curves of *N. crassa* can in theory evolve to have nearly any shape provided that appropriate selection gradients exist. Whether such selection gradients occur in nature is another matter. However, it seems more plausible that if there would be selection for increased growth at higher temperatures, evolutionary response will happen by increasing the overall elevation of the performance curve, which was the line of highest evolvability.

Revealing the genetic basis of performance curve variation is a topic for future studies, and would allow investigating whether trade-offs exists at the level of specific alleles. We are pursuing this question in future work.

AUTHOR CONTRIBUTIONS

The study was conceived by IK and TK; experimental design by IK, NNM, TK, and KS; experiments and data collection performed by NNM, KS, PAMS, and IK; data analysis by IK, NNM, and KS; manuscript was written by IK, with input from all other authors.

ACKNOWLEDGMENTS

This study was funded by grants from Emil Aaltonen foundation and Ella & Georg Ehrnrooth foundation to IK and Academy of Finland Research Fellowships to IK (no. 321584) and TK (no. 278751). We would like to thank Matthieu Bruneaux for comments on the manuscript.

DATA ARCHIVING

The data and analysis scripts have been deposited to data Dryad: <https://doi.org/10.5061/dryad.pk0p2ngk9>.

LITERATURE CITED

- Anderson, J. L., B. P. S. Nieuwenhuis, and H. Johannesson. 2018. Asexual reproduction and growth rate: independent and plastic life history traits in *Neurospora crassa*. *ISME J.* 13:780–788.
- Angilletta, M. J., R. S. Wilson, C. A. Navas, and R. S. James. 2003. Tradeoffs and the evolution of thermal reaction norms. *Trends Ecol. Evol.* 18:234–240.
- Araújo, M. B., F. Ferri-Yáñez, F. Bozinovic, P. A. Marquet, F. Valladares, and S. L. Chown. 2013. Heat freezes niche evolution. *Ecol. Lett.* 16:1206–1219.
- Arcus, V. L., E. J. Prentice, J. K. Hobbs, A. J. Mulholland, M. W. Van der Kamp, C. R. Pudney, E. J. Parker, and L. A. Schipper. 2016. On the temperature dependence of enzyme-catalyzed rates. *Biochemistry* 55:1681–1688.
- Ashrafi, R., M. Bruneaux, L.-R. Sundberg, K. Pulkkinen, J. Valkonen, and T. Ketola. 2018. Broad thermal tolerance is negatively correlated with virulence in an opportunistic bacterial pathogen. *Evol. Appl.* 11:1700–1714.
- Bennett, A. F., R. E. Lenski, and J. E. Mittler. 1992. Evolutionary adaptation to temperature. I. Fitness responses of *Escherichia coli* to changes in its thermal environment. *Evolution* 46:16–30.
- Bonini, B. M., M. J. Neves, J. A. Jorge, and H. F. Terenzi. 1995. Effects of temperature shifts on the metabolism of trehalose in *Neurospora crassa* wild type and a trehalase-deficient (*tre*) mutant. Evidence against the participation of periplasmic trehalase in the catabolism of intracellular trehalose. *Biochim. Biophys. Acta* 1245:339–347.
- Bürkner, P.-C. 2018. Advanced Bayesian multilevel modeling with the R package brms. *R J.* 10:395–411.
- Carpenter, B., A. Gelman, M. Hoffman, D. Lee, B. Goodrich, M. Betancourt, M. Brubaker, J. Guo, P. Li, and A. Riddell. 2017. Stan: a probabilistic programming language. *J. Stat. Softw.* 76:1–32.
- Castañeda, L. E., V. Romero-Soriano, A. Mesas, D. A. Roff, and M. Santos. 2019. Evolutionary potential of thermal preference and heat tolerance in *Drosophila subobscura*. *J. Evol. Biol.* 32:818–824.
- Colinet, H., J. Overgaard, E. Com, and J. G. Sørensen. 2013. Proteomic profiling of thermal acclimation in *Drosophila melanogaster*. *Insect Biochem. Mol. Biol.* 43:352–365.
- Davies, J., and D. Davies. 2010. Origins and evolution of antibiotic resistance. *Microbiol. Mol. Biol. Rev.* 74:417–433.
- Davis, R. H., and F. J. de Serres. 1970. Genetic and microbiological research techniques for *Neurospora crassa*. *Methods Enzymol.* 17:79–143.
- Deutsch, C. A., J. J. Tewksbury, R. B. Huey, K. S. Sheldon, C. K. Ghalambor, D. C. Haak, and P. R. Martin. 2008. Impacts of climate warming on terrestrial ectotherms across latitude. *Proc. Natl. Acad. Sci.* 105:6668–6672.
- Dillon, M. E., G. Wang, and R. B. Huey. 2010. Global metabolic impacts of recent climate warming. *Nature* 467:704–706.
- Ellison, C. E., C. Hall, D. Kowbel, J. Welch, R. B. Brem, N. L. Glass, and J. W. Taylor. 2011. Population genomics and local adaptation in wild isolates of a model microbial eukaryote. *Proc. Natl. Acad. Sci.* 108:2831–2836.
- Feder, M. E., and G. E. Hofmann. 1999. Heat-shock proteins, molecular chaperones, and the stress response: evolutionary and ecological physiology. *Annu. Rev. Physiol.* 61:243–282.
- Fragata, I., M. Lopes-Cunha, M. Bárbaro, B. Kellen, M. Lima, G. S. Faria, S. G. Seabra, M. Santos, P. Simões, and M. Matos. 2016. Keeping your options open: maintenance of thermal plasticity during adaptation to a stable environment. *Evolution* 70:195–206.
- Glatz, A., A.-M. Pilbat, G. L. Németh, K. Vince-Kontár, K. Jösvay, A. Hunya, A. Udvardy, I. Gombos, M. Péter, G. Balogh, et al. 2015. Involvement of small heat shock proteins, trehalose, and lipids in the thermal stress management in *Schizosaccharomyces pombe*. *Cell Stress Chaperones* 21:327–338.
- Gunderson, A. R., and J. H. Stillman. 2015. Plasticity in thermal tolerance has limited potential to buffer ectotherms from global warming. *Proc. R. Soc. Lond. B* 282:20150401.
- Guy, C. L., N. Plesofsky-Vig, and R. Brambl. 1986. Heat shock protects germinating conidiospores of *Neurospora crassa* against freezing injury. *J. Bacteriol.* 167:124–129.
- Hansen, T. F., and D. Houle. 2008. Measuring and comparing evolvability and constraint in multivariate characters. *J. Evol. Biol.* 21:1201–1219.
- Hill, W. G., M. E. Goddard, and P. M. Visscher. 2008. Data and theory point to mainly additive genetic variance for complex traits. *PLoS Genet.* 4:e1000008.
- Hochachka, P. W., and G. N. Somero. 2002. *Biochemical adaptation*. Oxford Univ. Press, New York.
- Houle, D. 1992. Comparing evolvability and variability of quantitative traits. *Genetics* 130:195–204.
- Huey, R. B., and J. G. Kingsolver. 1989. Evolution of thermal sensitivity of ectotherm performance. *Trends Ecol. Evol.* 4:131–135.
- . 1993. Evolution of resistance to high temperature in ectotherms. *Am. Nat.* 142:S21–S46.
- IPCC. 2013. Summary for policymakers. Pp. 1–30 in T. F. Stocker, D. Qin, G.-K. Plattner, M. Tignor, S. K. Allen, J. Boschung, A. Nauels, Y. Xia, V. Bex, and P. M. Midgley, eds. *Climate change 2013—the physical science basis: contribution of working group I to the fifth assessment report of the intergovernmental panel on Climate Change*. Cambridge Univ. Press, Cambridge. Available at www.climatechange2013.org.
- Izem, R., and J. Kingsolver. 2005. Variation in continuous reaction norms: quantifying directions of biological interest. *Am. Nat.* 166:277–289.
- Jacobson, D. J., J. R. Dettman, R. I. Adams, C. Boesl, S. Sultana, T. Roenneberg, M. Merrow, M. Duarte, I. Marques, A. Ushakova, et al. 2006. New findings of *Neurospora* in Europe and comparisons of diversity in temperate climates on continental scales. *Mycologia* 98:550–559.
- Kassen, R. 2002. The experimental evolution of specialists, generalists, and the maintenance of diversity. *J. Evol. Biol.* 15:173–190.
- Ketola, T., L. Mikonranta, J. Zhang, K. Saarinen, A.-M. Örmälä, V.-P. Friman, J. Mappes, and J. Laakso. 2013. Fluctuating temperature leads to evolution of thermal generalism and preadaptation to novel environments. *Evolution* 67:2936–2944.
- Ketola, T., and K. Saarinen. 2015. Experimental evolution in fluctuating environments: tolerance measurements at constant temperatures incorrectly predict the ability to tolerate fluctuating temperatures. *J. Evol. Biol.* 28:800–806.
- Klepsatel, P., M. Gáliková, N. De Maio, C. D. Huber, C. Schlötterer, and T. Flatt. 2013. Variation in thermal performance and reaction norms among populations of *Drosophila melanogaster*. *Evolution* 67:3573–3587.
- Knies, J. L., R. Izem, K. L. Supler, J. G. Kingsolver, and C. L. Burch. 2006. The genetic basis of thermal reaction norm evolution in lab and natural phage populations. *PLOS Biol.* 4. <https://doi.org/10.1371/journal.pbio.0040201>.
- Knies, J. L., J. G. Kingsolver, and C. L. Burch. 2009. Hotter is better and broader: thermal sensitivity of fitness in a population of bacteriophages. *Am. Nat.* 173:419–430.
- Krenek, S., T. U. Berendonk, and T. Petzoldt. 2011. Thermal performance curves of *Paramecium caudatum*: a model selection approach. *Eur. J. Protistol.* 47:124–137.
- Kronholm, I., H. Johannesson, and T. Ketola. 2016. Epigenetic control of phenotypic plasticity in the filamentous fungus *Neurospora crassa*. *Genes Genomes Genetics* 6:4009–4022.
- Kronholm, I., T. Ormsby, K. J. McNaught, E. U. Selker, and T. Ketola. 2020. Marked *Neurospora crassa* strains for competition experiments

- and Bayesian methods for fitness estimates. *Genes Genomes Genetics* 10:1261–1270.
- Latimer, C. A. L., B. R. Foley, and S. F. Chenoweth. 2015. Connecting thermal performance curve variation to the genotype: a multivariate QTL approach. *J. Evol. Biol.* 28:155–168.
- Le Vinh, Thuy, J., J. M. VandenBrooks, and M. J. Angilletta. 2016. Developmental plasticity evolved according to specialist–generalist trade-offs in experimental populations of *Drosophila melanogaster*. *Biol. Lett.* 12:20160379.
- Logan, M. L., J. D. Curlis, A. L. Gilbert, D. B. Miles, A. K. Chung, J. W. McGlothlin, and R. M. Cox. 2018. Thermal physiology and thermoregulatory behaviour exhibit low heritability despite genetic divergence between lizard populations. *Proc. R. Soc. B* 285:20180697. <https://royalsocietypublishing.org/doi/abs/10.1098/rspb.2018.0697>.
- Logan, M. L., I. A. Minnaar, K. M. Keegan, and S. Clusella-Trullas. 2020. The evolutionary potential of an insect invader under climate change. *Evolution* 74:132–144.
- Lynch, M. and B. Walsh. 1998. *Genetics and analysis of quantitative traits*. Sinauer Associates, Sunderland.
- Maclean, H. J., J. G. Sørensen, L. V. Kristensen, T. N., K. Beedholm, V. Kellermann, and J. Overgaard. 2019. Evolution and plasticity of thermal performance: an analysis of variation in thermal tolerance and fitness in 22 drosophila species. *Phil. Trans. R. Soc. B* 374:20180548.
- Mäki-Tanila, A., and W. G. Hill. 2014. Influence of gene interaction on complex trait variation with multilocus models. *Genetics* 198:355–367.
- Manenti, T., V. Loeschcke, N. N. Moghadam, and J. G. Sørensen. 2015. Phenotypic plasticity is not affected by experimental evolution in constant, predictable or unpredictable fluctuating thermal environments. *J. Evol. Biol.* 28:2078–2087. <http://doi.org/10.1111/jeb.12735>.
- Martin, C. E., D. Siegel, and L. R. Aaronson. 1981. Effects of temperature acclimation on *Neurospora* phospholipids fatty acid desaturation appears to be a key element in modifying phospholipid fluid properties. *Biochim. Biophys. Acta* 665:399–407.
- Martins, F., L. Kruuk, J. Llewelyn, C. Moritz, and B. Phillips. 2019. Heritability of climate-relevant traits in a rainforest skink. *Heredity* 122:41–52.
- McCluskey, K., A. Wiest, and M. Plamann. 2010. The fungal genetics stock center: a repository for 50 years of fungal genetics research. *J. Biosci.* 35:119–126.
- McElreath, R. 2015. *Statistical rethinking—a Bayesian course with examples in R and Stan*. CRC Press, New York.
- Merilä, J., and A. P. Hendry. 2014. Climate change, adaptation, and phenotypic plasticity: the problem and the evidence. *Evol Appl* 7:1–14.
- Mohsenzadeh, S., W. Saupe-Thies, G. Steier, T. Schroeder, F. Fracella, P. Ruoff, and L. Rensing. 1998. Temperature adaptation of house keeping and heat shock gene expression in *Neurospora crassa*. *Fungal Genet. Biol.* 25:31–43.
- Morrissey, M. B., L. E. B. Kruuk, and A. J. Wilson. 2010. The danger of applying the breeder's equation in observational studies of natural populations. *J. Evol. Biol.* 23:2277–2288.
- Palma-Guerrero, J., C. R. Hall, D. Kowbel, J. Welch, J. W. Taylor, R. B. Brem, and N. L. Glass. 2013. Genome wide association identifies novel loci involved in fungal communication. *PLoS Genet.* 9:e1003669.
- W. Piper, P. 1993. Molecular events associated with acquisition of heat tolerance by the yeast *Saccharomyces cerevisiae*. *FEMS Microbiology Reviews* 11:339–355.
- Plesofsky-Vig, N., and R. Brambl. 1985. Heat shock response of *Neurospora crassa*: Protein synthesis and induced thermotolerance. *J. Bacteriol.* 162:1083–1091.
- Powles, S. B., and Q. Yu. 2010. Evolution in action: plants resistant to herbicides. *Annu. Rev. Plant Biol.* 61:317–347.
- R Core Team. 2019. R: a language and environment for statistical computing. R Foundation for Statistical Computing, Vienna, Austria. Available at <http://www.R-project.org>.
- Roche, C. M., J. J. Loros, K. McCluskey, and N. L. Glass. 2014. *Neurospora crassa*: looking back and looking forward at a model microbe. *Am. J. Bot.* 101:2022–2035.
- Romero-Olivares, A. L., J. W. Taylor, and K. K. Treseder. 2015. *Neurospora discreta* as a model to assess adaptation of soil fungi to warming. *BMC Evol. Biol.* 15:198.
- Savage, V., J. Gillooly, J. Brown, G. West, and E. Charnov. 2004. Effects of body size and temperature on population growth. *Am. Nat.* 163:429–441.
- M Scheiner, S. 1993. Genetics and evolution of phenotypic plasticity. *Annu. Rev. Ecol. Syst.* 24:35–68.
- Schluter, D. 1996. Adaptive radiation along genetic lines of least resistance. *Evolution* 50:1766–1774.
- M Schulte, P. 2015. The effects of temperature on aerobic metabolism: towards a mechanistic understanding of the responses of ectotherms to a changing environment. *J. Exp. Biol.* 218:1856–1866.
- Sinclair, B. J., K. E. Marshall, M. A. Sewell, D. L. Levesque, C. S. Willett, S. Slotsbo, Y. Dong, C. D. G. Harley, D. J. Marshall, B. S. Helmuth, et al. 2016. Can we predict ectotherm responses to climate change using thermal performance curves and body temperatures? *Ecol. Lett.* 19:1372–1385.
- Sørensen, J. G., T. N. Kristensen, and V. Loeschcke. 2003. The evolutionary and ecological role of heat shock proteins. *Ecol. Lett.* 6:1025–1037.
- Sørensen, J. G., C. R. White, G. A. Duffy, and S. L. Chown. 2018. A widespread thermodynamic effect, but maintenance of biological rates through space across life's major domains. *Proc. Biol. Sci.* 285:20181775.
- Stinchcombe, J. R., R. Izem, M. S. Heschel, B. V. McGoey, and J. Schmitt. 2010. Across-environment genetic correlations and the frequency of selective environments shape the evolutionary dynamics of growth rate in *Impatiens capensis*. *Evolution* 64:2887–2903.
- Turner, B. C., D. D. Perkins, and F. A. 2001. *Neurospora* from natural populations: a global study. *Fungal Genet. Biol.* 32:67–92.
- Tüzün, N., and R. Stoks. 2018. Evolution of geographic variation in thermal performance curves in the face of climate change and implications for biotic interactions. *Curr. Opin. Insect Sci.* 29:78–84.
- Vehtari, A., A. Gelman, and J. Gabry. 2017. Practical bayesian model evaluation using leave-one-out cross-validation and WAIC. *Stat. Comput.* 27:1413–1432.
- Venables, W. N., and B. D. Ripley. 2002. *Modern applied statistics with S*. 4th ed. Springer, New York.
- C Whitlock, M. 1996. The red queen beats the jack-of-all-trades: the limitations on the evolution of phenotypic plasticity and niche breadth. *Am. Nat.* 148:S65–S77.

Associate Editor: K. McGuigan
 Handling Editor: D. Hall

Supporting Information

Additional supporting information may be found online in the Supporting Information section at the end of the article.

Figure S1 A) Phenotypic means for each genotype, those genotypes that were removed from the thermodynamic analysis as outliers are colored red.

Figure S2 Example MCMC traceplots for genetic standard deviations of growth rates in different temperatures in the multivariate model.

Figure S3 Illustration on how selection differential and selection gradient generate different responses to selection. Top row: selection based on selection differentials.

Figure S4 Selection for increased growth rate in a single temperature.

Figure S5 Selection for increased growth rate in two temperatures.

Figure S6 Selection for increased growth rate in three temperatures.

Table S1 List of strains. Column origin indicates whether strain was sampled from a natural population or if it was from a family obtained by crossing two natural strains.